Combining Electrochemistry and Metallurgy for New Electrode Designs in Li-Ion Batteries

S. Grugeon,[†] S. Laruelle,[†] L. Dupont,[†] F. Chevallier,[†] P. L. Taberna,[‡] P. Simon,[‡] L. Gireaud,[†] S. Lascaud,[§] E. Vidal,[§] B. Yrieix,[§] and J.-M. Tarascon*[,†]

LRCS-UMR 6007, Université de Picardie Jules Verne, 33 rue Saint-Leu, 80039 Amiens, France, CIRIMAT-UMR 5085, Université Paul Sabatier, Bât. 2R1-118, route de Narbonne, 31062 Toulouse Cedex 4, France, and EDF R&D, avenue des renardières, Ecuelles, 77818 Moret-sur-Loing Cedex, France

Received June 2, 2005. Revised Manuscript Received August 3, 2005

To benefit from the large electrochemical capacity advantages offered by Li-driven conversion reactions and to overcome poor kinetics, a new electrode configuration concept is reported. The originality of this electrode design is nested in metallurgical aspects of stainless steel, namely, the appearance of temperature-driven surface microstructures that enable the growth of a nanostructured, electrochemically active, chromium-rich oxide surface layer in close contact with a current collector. The thickness of the oxide layer can reach hundreds of nanometers and is shown to be rooted in the preferential migration of Cr toward the sample surface. We further show that chemical etching of the stainless steel surface, prior to high-temperature annealing, enables reversible capacities as high as 750 mAh/g of chromium-rich oxide for at least 800 cycles. On the basis of modeling, several scenarios involving stainless steel/chromium-based oxides current collectors of various porosities show how this new electrode configuration could boost the electrode capacity beyond that of today's carbon negative electrodes used in Li-ion cells by a factor of 2 or 3.

Introduction

Our society's increasing dependence on oil, combined with global warming and pollution in our cities, has conspired to make renewable energy a worldwide imperative for the upcoming years. As a result, there will be a far greater need for electrical energy storage to balance supply and demand since neither the wind blows nor the sun shines on demand! Meeting such an electrical energy storage challenge is a critical issue and one for which rechargeable lithium batteries have an important potential impact. Although widely used in most of today's power sources electronics, the Li-ion battery technology is currently not cost-competitive for such large-scale applications alluded to above. Breakthroughs in materials and new concepts are all essential if these systems are ever to satisfy increasing worldwide demands.

Today, rechargeable Li-ion batteries operate by an electrochemical process that involves intercalation reactions that, whatever the insertion/deinsertion electrode materials used, are limited to the insertion of one Li per 3d-metal. One way to circumvent this intrinsic limitation and achieve higher capacities would be the use of electrode materials in which the metal-redox oxidation state could reversibly change by more than one unit (M^{n+m}/M^{n+}, $m > 1$). A few research teams have explored new routes that have led to promising results.[1−3] For instance, our group recently reported reversible Li electrochemically driven CoO → Co conversion process involving a $2e^-$ reversible charge transfer per 3d-metal.[4−10] Such conversion reactions can lead to impressive capacity gains when involving $3e^-$ (Cr_2O_3) or $4e^-$ (RuO_2)[11] per d-metal and, best of all, they can also occur at voltages ranging from 0.5 V (Cr_2O_3) to 3 V (FeF_3) versus Li/Li^+.[12] Needless to say, for binary oxides to be used as negative electrodes in Li-ion cells, we need to select the ones that react toward Li at lower potentials. Among the best oxides, in terms of potential, are in order of merit $Cr_2O_3 > Mn_2O_3 > Fe_2O_3$, as previously deduced from thermodynamics calculations.[13]

Although the introduction of such conversion electrode materials in Li-ion batteries might seem an attractive scenario, implementation is beset with formidable technical difficulties such as charge/discharge transfer limitations associated with the poor electronic properties of binary

* Corresponding author. E-mail: jean-marie.tarascon@sc.u-picardie.fr.
[†] Université de Picardie Jules Verne.
[‡] Université Paul Sabatier.
[§] EDF R&D.

(1) Scrosati, B. *Nature* **1995**, *373*, 557.
(2) Tarascon, J.-M.; Armand, M. *Nature* **2001**, *414*, 359.
(3) Waklhara, W.; Yamamoto, O. *Advances in Lithium-ion batteries*; Kodansha-Wiley-VCH: Wenheim, Germany, 1998.
(4) Poizot, P.; Laruelle, S.; Grugeon, S.; Dupont, L.; Tarascon, J.-M. *Nature (London)* **2000**, *407*, 496.
(5) Dedryvère, R.; Laruelle, S.; Grugeon, S.; Poizot, P.; Gonbeau, D.; Tarascon, J.-M. *Chem. Mater.* **2004**, *16*, 1056.
(6) Poizot, P.; Laruelle, S.; Grugeon, S.; Tarascon, J.-M. *J. Electrochem. Soc.* **2002**, *149*, A1212.
(7) Laruelle, S.; Grugeon, S.; Poizot, P.; Dollé, M.; Dupont, L.; Tarascon, J.-M. *J. Electrochem. Soc.* **2002**, *149*, A627.
(8) Grugeon, S.; Laruelle, S.; Herrera-Urbina, R.; Dupont, L.; Poizot, P.; Tarascon, J.-M. *J. Electrochem. Soc.* **2001**, *148*, A285.
(9) Grugeon, S.; Laruelle, S.; Dupont, L.; Tarascon, J.-M. *Solid State Sci.* **2003**, *5*, 895.
(10) Debart, A.; Dupont, L.; Poizot, P.; Leriche, J.-B.; Tarascon, J.-M. *J. Electrochem. Soc.* **2001**, *148*, A1266.
(11) Balaya, P.; Li, H.; Kienle, L.; Maier, J. *Adv. Funct. Mater.* **2000**, *13*, 621.
(12) Li, H.; Balaya, P.; Maier, J. *J. Electrochem. Soc.* **2004**, *151*, A1878.
(13) Poizot, P.; Laruelle, S.; Grugeon, S.; Tarascon, J-M. *J. Electrochem. Soc.* **2002**, *149*, A1212.

10.1021/cm0511825 CCC: $30.25
Published on Web 09/09/2005

oxides. Thus, unless there is a drastic advance in electrode design/configuration, the concept of conversion reactions will remain an unlikely scenario.

Aware of such charge-transfer limitations, we embarked on a study of electrode (e.g., current collector/oxide interface) designs that could efficiently marry the current collectors with the binary oxides so as to utilize the capacity gains associated with conversion reactions. Aiming towards this goal, numerous approaches were tried such as the elaboration of Cr_2O_3−C electrode composites,[14] the growth of Cr_2O_3 thin film on various substrates, and the heat treatment of various metal current collectors. Among them we found, as reported herein, an attractive solution that consists in using a specially heat-treated stainless steel current collector as the electrochemically active electrode material. Through a survey of various parameters, such as the annealing temperature and the annealing time, combined with metallurgy considerations for the selection of the most suitable stainless steel formulation, nanotextured electrodes having large capacities and outstanding cycling performances versus Li (more than 800 cycles) were achieved. To set the scene, the paper starts with the growth and electrochemical performances of Cr_2O_3 thin films. The elaboration and physical and electrochemical characterization of nanostructured stainless steel current will then be presented and will be followed by a last section devoted to a preliminary modeling approach.

Growth of Cr_2O_3 Thin Film. Chromium oxide thin films were deposited at room temperature by ablating a pure polycrystalline chromium target under a controlled 5×10^{-2} oxygen pressure by means of a pulsed KrF excimer laser (Lambda physic, Complex 102, $\lambda = 248$ nm) on a 1.6-cm diameter titanium polished disk. Deposition times varied from 10 min to 6 h with a repetition rate of 10 Hz and a laser beam average fluency of 1 to 2 J/cm^2. To obtain a uniform ablation over the target surface, the target was continuously rotated. Using such conditions, films with thicknesses from about 40 nm to about 500 nm, as determined by means of a TENCOR P-2 Long Scan profilometer, were obtained. Independently of the thicknesses, the films are amorphous, and a post-annealing at 400 °C was necessary to promote crystallization and to obtain films having the Cr_2O_3 corundum structure, as deduced by X-ray measurements, performed on a Philips PW1729 diffractometer using Cu K_α monochromatic radiation.

The films were tested for their electrochemical behavior using coin cells (standard 2035-size) that were assembled in an argon-filled drybox. The positive thin film Cr_2O_3 disk was separated from a lithium disk used as the negative electrode by a borosilicate microfiber (Millipore) film impregnated with 0.1 mL of a $LiPF_6$ (1 M) in EC-DMC (1−1 weight ratio) solution. The electrochemical tests were carried out using a Mac pile system (Biologic S. A., Claix, France) in a galvanostatic mode at 55 °C. Such a temperature was purposely selected to fully use the capacity of the Cr_2O_3-based electrode that is concentrated near zero volt versus Li^0/Li^+ during its first discharge and therefore is not easily reachable at room temperature. All reported potential values

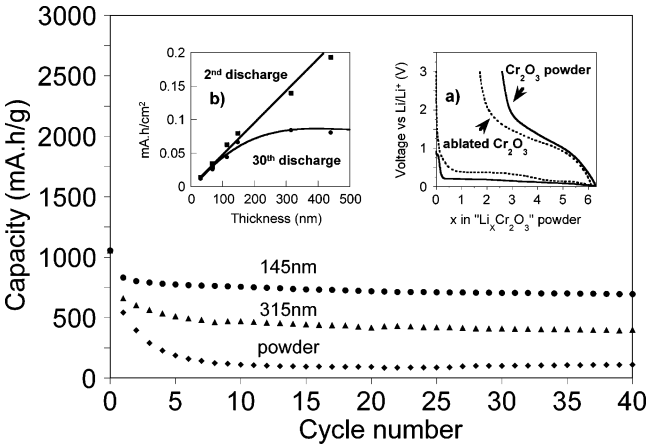

Figure 1. The capacity retention of ablated Cr_2O_3/Li cells is plotted as a function of the cycles number and is compared with the capacity decay of a carbon containing Cr_2O_3/C composite (85/15 wt %)/Li cell. All of the cells were cycled between 0.02 and 3 V at a rate of 0.015 mA/cm^2 and C/40 (1 Li^+ in 7 h) for the thin film and powder electrodes, respectively. In **(a)** the voltage curve (dots) for an ablated Cr_2O_3/Li cell cycled between 0.02 and 3 V is compared to that of a Cr_2O_3 powder with 15 wt % carbon black (SP from MMM, Belgium)/Li cell (solid line). In **(b)** the 2nd and 30th discharge capacity values for the above Cr_2O_3 thin films-based cells are plotted as a function of the film thickness.

are given versus Li^0/Li^+ and the rate is calculated by supposing the whole active material being reduced during the first discharge. Figure 1 (inset a) shows a potential/composition curve obtained for ablated Cr_2O_3/Li cell using film of 65-nm thickness, cycled at a nominal C/3 rate (C being defined as $2Li^+$/h) in the 0.02−3 V potential window. The first discharge is characterized by the reaction of 3Li/Cr at low potential with the hints of two plateaus appearing near 0.35 and 0.2 V. These potentials are close to the one observed for Cr_2O_3 powders (1−3 μm particles) with 15 wt % carbon black (SP from MMM, Belgium) tested in Swagelok cells at a C/40 rate. Upon subsequent charges, the voltage smoothly and continuously increases from 0.02 to 3 V with an overall Li release of 4.3 Li implying a 28% irreversible capacity, with therefore an overall reversible capacity of 750 mAh/g. Such results do not come as a surprise, but they simply suggest a classical conversion reaction process ($Cr_2O_3 + 6Li^+ + 6e^- \rightarrow 2Cr^0 + 3Li_2O$) with the reduction of Cr^{3+} in Cr^0. The observed initial reversible capacity is nested in the incompleteness of the re-oxidation reaction because we do not convert back to Cr^{3+} but to Cr^{2+} (CrO) as separately deduced by HRTEM.

The voltage−composition traces were independent of film thickness. The films were tested for their capacity retention (Figure 1). The variation of the capacity of each cell after the 2nd and 30th cycles is plotted as a function of the thickness of the films (Figure 1, inset b). The second discharge capacity increases linearly as a function of the film thickness up to about 300 nm and then slightly deviates for thicknesses greater than 300 nm. This contrasts with the 30th discharge capacity that increases linearly up to about 150−175 nm and levels off beyond. Films having a thickness below 175 nm were found to nicely sustain their capacity upon cycling up to a few hundred cycles. For the thicker films, we note a rapid capacity decay, which worsens with increasing the thickness, indicative of a decrease in the reversibility of the conversion reaction, thus implying that

(14) Hu, J.; Li, H.; Huang, X. *Electrochem. Solid-State Lett.* **2005**, *8*, A66.

an increasing amount of electrode material becomes inactive upon cycling. The capacity decay is more catastrophic for powders as one could have expected owing to their large particle size (1−3 μm). Both kinetic limitations and material degradation on cycling are most likely at the origin of this capacity retention/film thickness dependence decay.

Charge/discharge kinetics are controlled by the cumulative effects of (a) the transport of ions and electrons from their respective sources to the surface of the storage material, (b) the electrochemical reaction at/across the surface, and (c) the solid-state diffusion within the storage material. Therefore, because films of all thicknesses can be fully utilized capacity-wise through the first two cycles, we cannot eliminate the existence of a progressive surface flaking process (e.g., particles becoming disconnected from the film surface during cycling). With such a process, the formed metallic Cr particles would become electronically disconnected and unavailable for cycling. Such a flaking effect is expected to be more pronounced for thicker films, as cohesion of the film particles weakens (e.g., the oxides particles far away from the substrate interface no longer sense the effect of the substrate). When the films are thin, we always maintain the electronic path owing to some tunnelling between the metallic particles. Such results are consistent with the previously reported[14] ability of cycling carbon-containing Cr_2O_3 powders versus Li/Li^+ and not carbon-free Cr_2O_3 powders, owing to the absence of electronic percolation.

Whatever the origin of this capacity fading, the main message conveyed by the thin film study is the feasibility of using such reversible conversion reactions without any carbon additives, if their thickness is $<\cong$175 nm. Therefore, increasing the electrochemically active electrode thickness is not a viable option to improve electrodes. Obviously, what one would like is to develop a large surface area current collector covered with 175 nm of Cr_2O_3. Having set the stage, we searched for different ways to prepare electrodes to maximize the surface area of the conversion reactions. As we report here, the most successful so far uses specific metallurgical aspects to design new electrochemically active current collectors. More specifically, we took advantage of the stainless steel compositions rich in Cr, Fe, and Mn for which oxides can reversibly react toward Li via conversion reactions.

Nanostructured SS Current Collector. *Chemical/Physical Characterizations.* Owing to the well-documented problems of corrosion in metallurgy leading to the formation of specific surface metal oxides, we decided to embark in studies aimed at the creation of large active surfaces on stainless steel current collectors. Our choice of stainless steel resided in its composition rich in Cr and Fe, and which oxides can reversibly react toward Li via conversion reactions. Our first experiments were conducted using stainless steel disks (SUS316L purchased from Hohsen Corporation) that support the positive electrochemically active materials in today's coin cells. The disk composition in metal elements reveals the presence of numerous elements in the following atomic ratio percentage (Cr: 17−19%, Ni: 12.5−15%, Mo: 2−3%, Mn: 1−2%, and Si: 0.5−1% and traces of others P, S, N). The disks were gradually heated under nitrogen with 10% hydrogen (high purity given with 5 ppm O_2) at 5 °C/min at temperatures ranging from 25 °C to 800 °C and were maintained for 13 h at this temperature prior to being cooled down (furnace turned off). The treated samples, slightly different in color with respect to the original ones (yellowish vs grayish), were transferred to an argon-filled drybox without exposure to air prior to characterization.

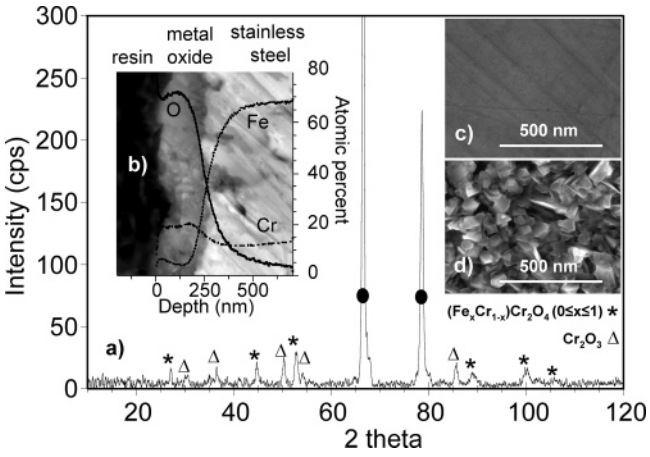

Figure 2. In **(a)** the X-ray diffraction pattern of a stainless steel current collector annealed at 700 °C for 13 h under a H_2/N_2 flow shown together with the SEM micrographs of a polished stainless steel disk (SUS316L) prior to **(c)** and after the heating treatment **(d)**. The SEM cross section of the same disk **(b)** clearly highlights the oxide layer forming at the stainless steel surface. As a guide to the reader, we reported the Fe, Cr, and O atomic percent variation through the oxide/stainless steel interface (as deduced from GD-OES measurements).

X-ray measurements of the high-temperature treated disks reveal the coexistence in equal proportion (Figure 2a) of two chromium-rich oxide phases: a chromite phase $(Fe_xCr_{1-x})Cr_2O_4$ ($0 \leq x \leq 1$) (accurate composition being determined by means of HRTEM) having the spinel structure and a sesquioxide type Cr_2O_3 phase having the corundum structure. The surface morphology and elemental composition of the disks were examined by means of a Philips XL 30 Field Emission Gun (FEG) coupled to an Oxford Link instrument for energy-dispersive X-ray spectroscopy (EDS). Analysis for composition of the sample surfaces showed a drastic difference between the initial and treated samples, going from 72, 18, and 10% in Fe, Cr, and Ni for the fresh sample to about 53, 37, and 10% for the treated sample, respectively. Figure 2c and d shows scanning electron micrographs of the SUS316L disk surface before and after its 700 °C thermal treatment. Drastic changes can be observed too. The smooth surface has turned into a rough one composed of uniformly distributed nanoparticles (<100 nm), poorly packed, implying that the thermal treatment has induced a porous nanostructured surface. The cross-sectional microscopy of the same treated stainless steel disk, after being embedded in a resin matrix, cut, and polished, shows the presence of a 250 ± 50 nm thick surface oxide layer (Figure 2b) consisting of densely packed nanoparticles within the core of the film. We will show that both the surface porosity and the particle size (50−100 nm) can be tuned by chemical and physical treatments to fall within the size range previously determined for good cycling performance.

Both SEM and X-ray studies strongly suggest that the thermal treatment promotes an enrichment of the surface in

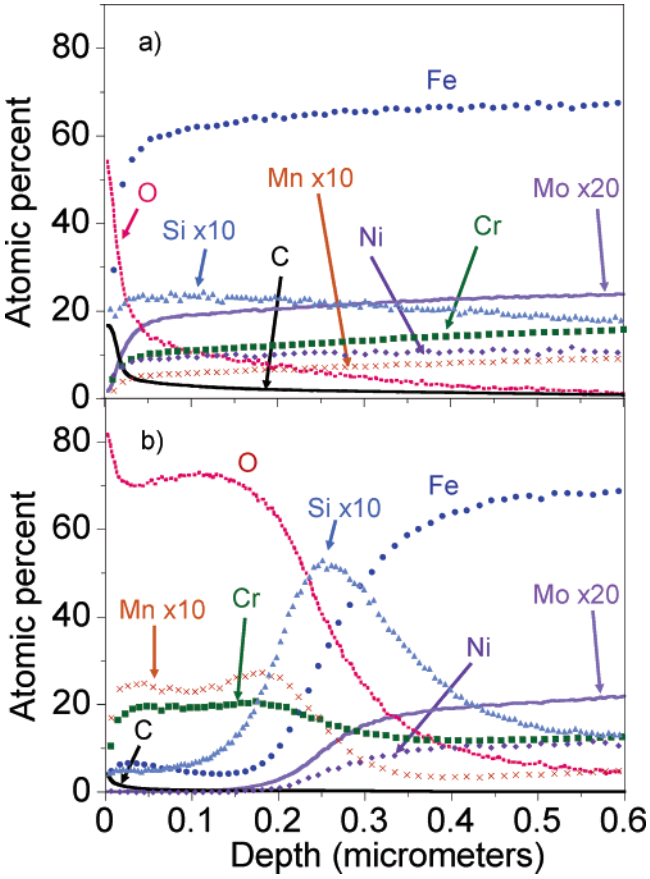

Figure 3. Quantitative depth profile analyses, as deduced from glow discharge optical emission spectrometry, for an as-made (a) and for a high-temperature (700 °C) treated stainless steel disk (SUS316L) (**b**). There is a depletion of Fe and Mo at the surface at the expense of a surface accumulation of O and Cr.

Cr at the expense of Fe but does not provide accurate information on the thickness of the formed oxide layers or on the depth dependence of the elemental composition. Quantitative elemental depth profiles of treated stainless steel samples were determined with glow discharge optical emission spectrometry (GD-OES)[15] using an LECO GDS-750A optical emission spectrometer. The average atomic percent of the various metallic elements together with O are plotted versus depth for both non-treated and thermally treated samples (Figure 3a and b). There are several noticeable differences with, namely, an oxide layer that is about 15−20 times thicker (250 nm) for the treated sample than for the non-treated sample. The oxygen is found to coexist over such a thickness with large amounts of Cr (20%) and moderate amounts of Fe (5%) and Mn (2%). In contrast, no Ni or Mo was present in this 250-nm oxide layer. Among other interesting features revealed by GD-OES analyses are (1) the enrichment of Si at the oxide/stainless steel interface as indicated by the maximum in the average percent Si content at about 250 nm and (2) a decrease in the surface carbon content for the treated sample as compared to the non-treated sample.

These results indicate that the thermal treatment promotes a migration of the metallic elements with surface enrichment of Cr at the expense of Fe and Ni. Chromium oxide being one of the most stable oxides, the freshly made Cr atoms will react with traces of oxygen present within the reducing gas to form the chromite phase. Overall, through this process, the most important reaction is an oxidation reaction. Cr scavenges O_2 from the impure H_2, whereas the rest of the 3d metals would be reduced by this same H_2/O_2 ppm combination. To check whether the thickness of the oxide layer depends, for a fixed reducing gas composition flow, on the treatment temperature, three samples were annealed for the same period (16 h) at three different temperatures 600, 700, and 800 °C. A GD-OES analysis of the samples indicated that the thickness of the oxide layer linearly increases from 100 to about 500 nm as the temperature is raised from 600−800 °C. Independently of the temperature, the Cr percentage remains constant within the oxide layer while the Mn percentage slightly increases from 1 (600 °C) to 5% (800 °C) while the Fe content decreases from 11 to 3.5

Electrochemical Characterization. The non-treated and treated stainless steel disks (SUS316L) were investigated for their electrochemical performance versus Li using coin cells hardware. The cells were cycled at 55 °C between 0.02 and 3 V at various rates. Lacking the exact amount of active material, we report capacities in mAh/cm^2. A typical voltage−composition curve for the treated sample is shown in Figure 4a. The curve is somewhat similar to that obtained for the Cr_2O_3 thin films (see Figure 1a), namely, a discharge trace being located near 0 V with a capacity of 0.16 mAh/cm^2 and a recharge that does not return to 0 mAh/cm^2 at 3 V but to 0.055 mAh/cm^2, leading to a total irreversible capacity of 33%, consistent with our inability to reoxidize Cr^0 to Cr^{3+} at 3 V.[14] Because our oxide layer is a mixture of Cr-based corundum and spinel structures, one might have expected some differences in the voltage−composition curve as compared to that of pure Cr_2O_3 thin films. To check this point, we prepared Fe-substituted $Fe(Fe_xCr_{1-x})_2O_4$ and $(Fe_xCr_{1-x})_2O_3$ ($0 \leq x \leq 0.2$) phases and tested their electrochemical behavior versus Li in Li/half cells. Their first discharge potential was found to remain within the 0.2−0.4 V discharge range, explaining the slight potential deviation between thin films and our treated stainless steel samples. The treated disk electrodes exhibit outstanding sustained capacity retention (Figure 4a inset), since more than 800 cycles can be achieved without any capacity loss. On the contrary, the slight increase in capacity observed upon cycling, which was enhanced with the cycling temperature,[16] is most likely indicative of an oxide layer slowly growing during continued charging. Finally, the non-treated sample shows no electrochemical capacity (Figure 4b).

The capacity retention of films, treated at 600, 700, and 800 °C, indicates an increase in capacity with increasing temperature (Figure 4b) consistent with the GD-OES results that have shown that the oxide layer thickness (Figure 4b inset), and therefore the amount of electrochemically active oxides, increases with the temperature. Upon the 30th cycle, we obtained capacities of 0.08, 0.13, and 0.2 mAh/cm^2 for

(15) Payling, R.; Jones, D.; Bengtson, A. *Glow Discharge Optical Emission Spectrometry*; John Wiley and Sons edition, 1997.

(16) Tarascon, J. M.; Grugeon, S.; Morcrette, M.; Laruelle, S.; Rozier, P.; Poizot. P. *C. R. Chim.* **2005**, *8*, 9.

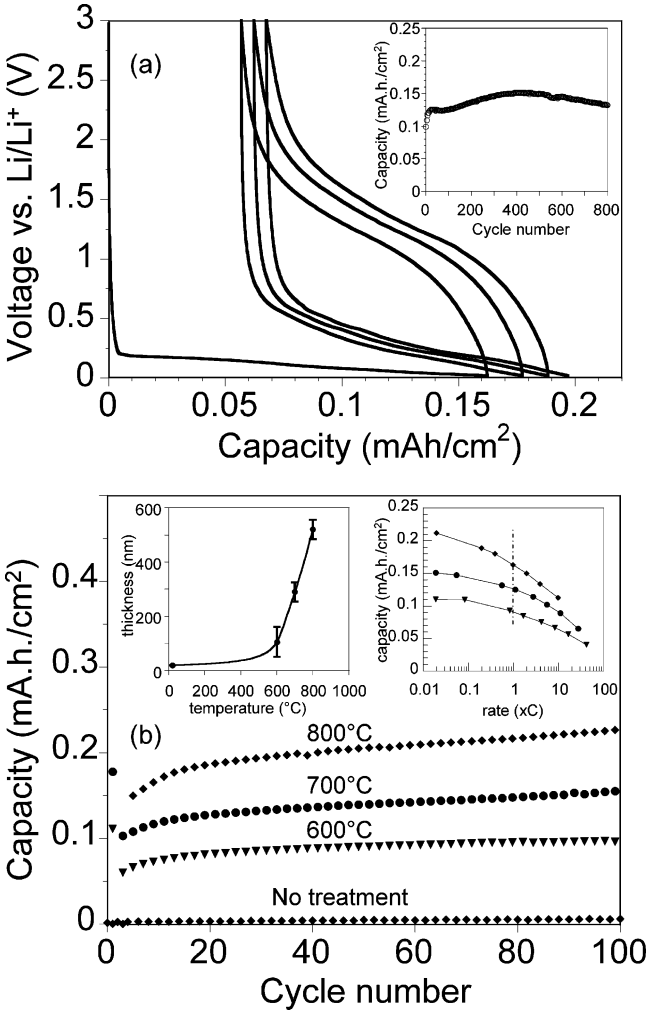

Figure 4. Typical charge/discharge voltage−capacity traces for a 700 °C treated SUS316L disk/Li cell are shown in **(a)** together with an inset of the cell capacity retention. The capacity retention measured on chromium based oxides/Li cells using as the positive electrodes stainless steel disks (SUS316L) treated at 600, 700, and 800 °C is plotted in **(b)** and is compared with the capacity retention of a non-treated sample. Left in the inset are the thicknesses, as deduced from GD-OES measurements, of the oxide layers present at the surface of the 600, 700, and 800 °C treated stainless steel disks and in the right are the power rate capabilities for the corresponding samples.

substrates having thickness surface layers of 100, 290, and 500 nm, respectively. This deviation from a linear law variation is most likely nested in the porosity of the grown oxide layer that differs with the temperature as well, so that a thicker layer may have a large porosity. An indirect way to estimate the porosity is to reconvert the thin film and stainless steel substrate data. We measured a capacity upon the second discharge of about 0.104 mAh/cm^2 for stainless steel films annealed at 700 °C and having an oxide layer estimated at 290 nm. From Figure 1 (inset b), we can deduce that such capacity can be obtained with 213-nm dense thin films. Thus, we deduce that the oxide layer formed at 700 °C has a porosity of about 27%. Interestingly, such films can be cycled as much as 800 times between 0.02 and 2.5 V (Figure 4a inset) with a slight capacity gain**.** The rate capabilities of the stainless steel disks treated at 600, 700, and 800 °C are shown in the upper right insert of Figure 4b. At 1C (dashed line), the output capacities of the 600, 700, and 800 °C treated films are 84, 86, and 76% of their initial capacities, respectively. This indicates that the thicker films (e.g., the 800 °C ones) have the poorest performances owing to kinetic limitations intrinsic to the Cr-based oxide active material.

Through the above studies, we have shown the positive attributes that metallurgy could bring to the field of energy storage via the development of temperature-driven nanostructures concomitant with the growth of oxide layers that enables an efficient utilization of conversion reaction. Therefore, to fully use such metallurgical assets, one must find other means to increase the current collector porosity. Indeed, corrosion resistance of stainless steel is reduced by open porosity[17,18] since porosity exposes a larger surface area to the environment. Thus, we investigated the possibility of corroding stainless steel disks prior to performing our high-temperature treatment under reducing atmosphere.

Physical and Electrochemical Characterization of Corroded Stainless Steel Disks. Stainless steel disks (SUS316L) (1.6-mm diameter, 0.5-mm thick, and containing 17% of Cr) were chemically treated at room temperature in the hope of enlarging the specific surface of the stainless steel plates. We used a previously reported chemical conversion treatment[19] listing three steps: (1) a cleaning in tetrahydrofuran, (2) a 5-min activation step in 5% vol sulfuric acid, and (3) a 25-min chemical oxidation in a suitable acid solution. The chemical bath was composed of 0.93 M of H_2SO_4, 0.0006 M of $Na_2S_2O_3$, and 0.05 M of C_3H_4O (propargylic alcohol). $Na_2S_2O_3$ and C_3H_4O play the role of activator and cathodic inhibitor, respectively. Aries et al.[20−21] previously demonstrated that such additives enable control of surface porosity in stainless steel. All the steps of this treatment were performed at room temperature except for the chemical oxidation that was conducted at 60 °C for either 5 or 20 min, leading to two samples denoted A and B, respectively. The SEM pictures collected for the A sample after the chemical pretreatment (Figure 5 inset) show a drastic surface morphology evolution with the appearance of a very porous surface. Afterward, the A and B samples were treated as before at 700 °C for 13 h under a H_2/N_2 reducing atmosphere. The high-temperature treatment was found to induce minor surface morphology changes with some evidence for iron grains growth**.** Further evidence for the chemically driven stainless steel porous surface was brought about by BET measurements performed using Krypton as the absorbing gas, which indicates an increase in the stainless steel surface porosity from 1 m^2/m^2 for the initial material to 6 m^2/m^2 and 13 m^2/m^2 for samples A and B, respectively. Interestingly, we measured that high-temperature heating treatment does not lead to any detectable changes in the sample porosity at least within the accuracy range of the measurements that is about 0.3 m^2/m^2.

(17) Matula, M.; Hyspecka, L.; Svoboda, M.; Vodarek, V.; Dagbert, C.; Galland, J.; Stonawska, Z.; Tuma, L. *Mater. Charact.* **2001**, *46*, 203.
(18) Otoro, E.; Pardo, A.; Utrilla, M. V.; Pérez, F. J.; Merino, C. *Corros. Sci.* 39, **1997**, *3*, 453.
(19) Labar, J. L. *Proc. Of EUREM 12*; Brno, L., Franck, Ciampor, F., Eds.; 1379 2000.
(20) Aries, L.; Alberich, L.; Roy, J.; Sotoul, J. *Electrochim. Acta* **1996**, *41* (18) 2799.
(21) Aries, L.; Roy, J. *Mater. Sci. Technol.* **1994**, *10*, 359.

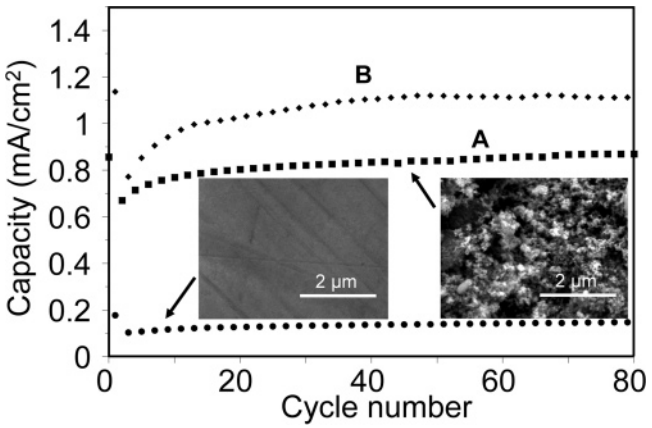

Figure 5. The capacity of a heat-treated (SUS316L) disk is compared to that of another similar disk that was purposely corroded through chemical means and then annealed at 700 °C in a reducing H_2/N_2 flow. The inset shows the change in sample microstructure as the result of the heating treatment.

The effect of the room-temperature surface treatment on the stainless steel electrode capacity is shown in Figure 5. While keeping the same high-temperature heating treatment, one notices that a 5-min chemical treatment (sample A) is sufficient to lead to a 5-fold increase in the electrode capacity (0.8 mAh/cm^2 for the chemical treated samples as compared to 0.16 mAh/cm^2 for the non-treated one). As expected, such capacities are dependent on the stainless steel porosity since the B samples (having a BET of 13 m^2/m^2) show a capacity of 1.1 mA/cm^2. One direction of the present studies is to focus on tuning the various parameters governing this chemical dissolution process to achieve the largest porosities. Finally, preliminary tests on commercial porous stainless steel disks (kindly given by EIF Society) have also been carried out, and their high potentiality as electrodes is demonstrated.

Modeling Approach. Overall, the objective of this study was the design of electrodes with an extremely high current collector/oxide interface contact to improve reaction kinetics. Such a surface contact requires highly porous electrodes so that the price paid in terms of dead volume can be recovered. Thus, at this point, a legitimate question is whether the proposed nanostructured and porous stainless steel electrode, aimed at countering kinetic limitations of conversion reactions, can successfully compete with today's classical insertion/deinsertion electrodes involving at most one electron per 3d-metal. To address this question and to gain insight into the relationship between various physical/chemical aspects of the porous, nanostructured, stainless steel/oxide current collector (nature and thickness of the oxide material, porosity, thickness of the electrode, etc.) and the resulting electrode capacities, we created an electrode modeling spreadsheet.

For reasons of comparison with today's carbon electrodes used in Li-ion cells, whose thickness is 160 μm of which 25 μm is the copper current collector, the thickness of our stainless steel electrode was fixed to equal 160 μm. We further assumed 1D homodispersed, longitudinal pores running perpendicular to the disk surface, whose depth, internal size, and interpore distances can be adjusted. Using this model, we can estimate how the electrode capacity would vary as a function of the electrode porosity, the oxide thickness layer, and the reversible capacities of the oxide materials. Two scenarios were considered using the optimal thickness of 250 nm deduced from thin film work. In the first case, the pore diameter and interpore distance were kept constant but the electrochemical capacity of the oxide layer

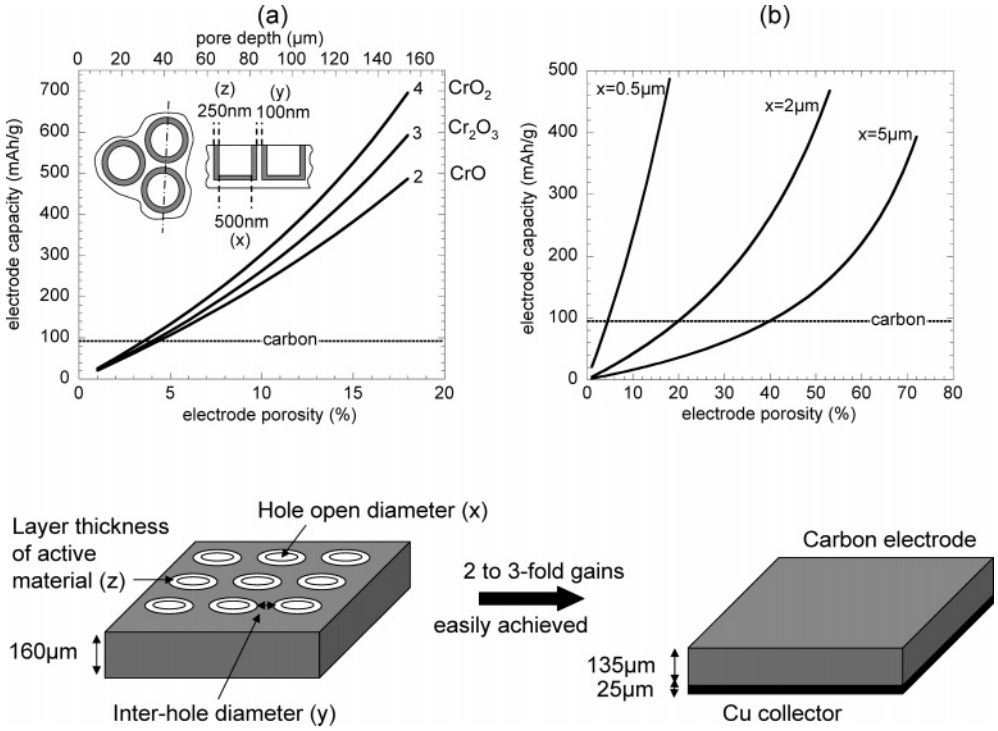

Figure 6. Estimates made, according to details given in the text, are shown **(**a**)** to sense the effect of the porosity of the stainless steel current collector and of the nature of the conversion reaction (e.g., involving either CrO (2e$^-$), Cr_2O_3 (3e$^-$), or CrO_2 (4e$^-$)) on the overall stainless steel electrode capacity and **(**b**)** to sense the effect of the porosity of the stainless steel current collector and of the pore diameter in the case of CrO and compare with today's state-of-the-art carbon negative electrodes used in Li-ion cells. Estimates were obtained using a modeling spreadsheet having various variable parameters (see text).

was varied from CrO ($2e^-$) and Cr_2O_3 ($3e^-$) to CrO_2 ($4e^-$) per 3d metal. In the second case, we fixed the electrochemical capacity of the oxide layer to $2e^-$ per 3d-metal but varied the pore diameter from 0.5 to 5 μm. The results of such calculations (electrode capacity as a function of its porosity) are plotted in Figure 6a and b for the two cases considered above together with the capacity of a 160-μm carbon electrode used in today's Li-ion cells that averages about 96 mAh/g of the total electrode weight (carbon + copper current collector). For either scenario, it can be deduced that the capacity of the overall nanostructured, porous, stainless steel electrode can exceed that of carbon. For instance, assuming both a $2e^-$ conversion reaction and a 0.5-μm pore diameter, we can reach capacities comparable to those of carbon with 5% porosity and achieve 4 times greater capacity for 15% porosity (Figure 6a). We are well aware that to be more realistic, the above calculation must be extended to a porous 3D network, and this will be done in the future. Therefore, such preliminary results have the merit of raising our awareness towards the benefits of designing porous nanostructured stainless steel electrodes. Great effort is being presently devoted toward optimizing the porous nanostructured electrode design to achieve the largest capacity enhancement.

Conclusions

Stainless steels are used in countless diverse applications, most of them requiring materials highly resistant against corrosion and therefore with a Cr content greater than 13%. Interestingly, we have reported their use in situations opposite to what they are designed for, since we purposely amplified their corrosion by a high-temperature treatment to promote the growth of Cr-based oxide at the surface of stainless steel current collectors. We believe such an oxide nucleation, concomitant with the migration of metallic elements, is the key to building an interface that provides both good adhesion of the oxide to the substrate and a suitable path for electron transport. Some of today's best lead acid[22] and Ni[23] electrodes have that aspect in common, although in those cases the formation was electrochemical. Using such a philosophy, we succeeded in preparing stainless steel/chromium-based oxide electrodes showing, in absence of any carbon additives, large and sustainable reversible capacities toward Li. Furthermore, we have described a way to enhance the electrode capacities by an order of magnitude by simply combining classical corrosion treatments, proper stainless steel, and our high-temperature annealing process. Finally, a simple electrode modeling approach suggests that such self-supported oxides/current collectors could offer substantial gains over today's carbon electrodes in terms of capacity gains. It is therefore important to realize that the chromium oxide-based electrodes, described herein, are not the best candidate to replace carbon electrodes owing to their charge/discharge curves that make their potential too high versus Li/Li+ to be totally useful, regardless of the capacity gains. We have demonstrated the principles but further materials advances are still needed to get the voltages of these conversion reactions to more suitable values. This is not an insurmountable task as we are presently surveying numerous families of materials reacting with Li though conversion reactions. Overall, we hope that this work, which highlights the benefits of combining both the fields of metallurgy and electrochemistry, will help to pave the way for further advances in the use of conversion reaction electrode designs that could lead to the next generation of Li-ion batteries.

Acknowledgment. The authors thank Science et Surface company for the GD-OES analyses, D.W Murphy for sound discussions, J-B. Leriche for technical help, and P. Alphonse for the BET surface area measurements.

CM0511825

(22) Koontz, D. E.; Feder, D. O.; Babusci, L. D.; Luer, H. J. *Bell Syst. Tech. J.* **1970**, *49*, 1253.
(23) Ho, K. C.; Jerne, J. *Electrochem. Eng. App.* 83, **1987**, *254*, 87.